

Multi-Parton Scattering Amplitudes via On-Shell Methods

CAROLA F. BERGER

*Center for Theoretical Physics, Massachusetts Institute of Technology,
Cambridge, MA 02139, USA*

DARREN FORDE

*Theory Division, CERN, CH-1211 Geneva 23, Switzerland,
NIKHEF Theory Group, Science Park 105, NL-1098 XG Amsterdam, The
Netherlands*

Key Words QCD, precision calculations, next-to-leading order, generalized unitarity, recursion relations

Abstract We present an overview of recent developments, based on on-shell techniques, in the calculation of multi-parton scattering amplitudes at one loop that are relevant for phenomenological studies at hadron colliders. These new on-shell methods make efficient use of the physical properties of the hard scattering, such as unitarity and factorization.

CONTENTS

Introduction	2
Structure of Amplitudes	4
<i>Notation and Color Decomposition</i>	4
<i>On-Shell Recursions at Tree Level</i>	6
<i>Structure of One-Loop Amplitudes</i>	8
Extraction of Integral Coefficients via Unitarity	8
<i>Generalized Unitarity in Four Dimensions</i>	9
<i>Extraction of Integral Coefficients at the Integrand Level</i>	13
<i>Rational Terms from D-Dimensional Generalized Unitarity</i>	16
On-Shell Recursion at One Loop	20
<i>Spurious Poles</i>	21
<i>Contribution from Infinity</i>	23
Conclusions and Outlook	24

1 Introduction

With the recent first collisions at the LHC we are entering a new era of discovery in particle physics. Colliding protons at very high energies makes the LHC a fertile environment for the production of high-multiplicity events. If we are to take full advantage of the discovery potential at high energy hadron colliders such as the Tevatron and the LHC, we need to have a precise understanding of the physics that will occur there. This necessitates computations of the Standard Model background, especially of QCD processes, to at least next-to-leading order (NLO) in the perturbative series.

Historically, the bottleneck in NLO computations has been the one-loop virtual contributions. Over the last few years rapid progress has been made in the development of new techniques for these one-loop computations. These advancements have been motivated both by a greater desire to understand the structure of scattering amplitudes as well as the need for improved efficiency and automation in the computation of one-loop matrix elements. These matrix elements are needed, for example, for the precise computation of many background processes at the LHC (see e.g. (1)). The ability to automate and “mass-produce” amplitudes requires approaches that are both numerically stable and straightforward to implement as an algorithm.

The standard approach to performing this class of computations has heavily relied upon Feynman diagram techniques. There have been many impressive results with this approach (see (1) and references therein; for example, cross sections for 6-point processes that have been computed via Feynman diagrammatic methods include (2)). However, Feynman diagrams suffer from two problems. For one, there is a factorial growth in the number of terms as the multiplicity of partons in the process increases. Furthermore, each Feynman diagram is gauge dependent. This means that there will be large cancellations between terms that combine to give the gauge-independent amplitudes. It is these two problems that make automated approaches using Feynman diagrams difficult as the number of partons increases.

Consequently, the focus of much recent progress has been to side-step these issues. On-shell recursion and unitarity methods work with gauge-independent amplitudes as building blocks instead of Feynman diagrams. It is these new techniques that we focus on in this review. An earlier review of these techniques was presented in (3). However, many of the details presented there have been superseded by even more efficient techniques which we present in the following.

In general, as we will explain in more detail below, a one-loop amplitude can be decomposed into a set of scalar box, triangle, bubble, and tadpole integrals, that is, integrals with four, three, two, or one loop propagators, respectively. These scalar integrals contain all the logarithmic and polylogarithmic dependence of the amplitude and are multiplied by rational coefficients. In addition, there are also

purely rational terms in the amplitude.

The original unitarity approach of (4) applied two-particle cuts in four dimensions and was used to produce many results (5). The terms containing (poly)logarithms and associated constants could all be computed via two-particle cuts. Terms with only a rational dependence on momentum invariants however could not be computed in this way and separate techniques were required (5). A systematic approach for the computation of these rational terms without the use of Feynman diagrams did not appear until a few years ago. The starting point for these developments were the recursion relations, developed at tree level by Britto et al. (BCFW) (6). An earlier version of a tree-level recursion relation was the off-shell Berends-Giele recursion (7). The proof of the BCFW on-shell recursion relations only relies upon the factorization properties of the amplitudes and on Cauchy's theorem. They could therefore be adapted to the more complicated problem of computing the rational parts of loop amplitudes (8,9). On-shell recursion for the rational parts of loop amplitudes was first used in an analytic context (9) and then further adapted into a numerical procedure (10).

At the same time, improvements to the original unitarity approach were also occurring. Brandhuber et al. used two-particle cuts with MHV vertices to compute certain sets of one-loop amplitudes (11). The application by Britto et al. of generalized unitarity (5,12) to the computation of box coefficients highlighted the benefits of examining not the one-loop integral as a whole, but its integrand. The work of Ossola, Papadopoulos and Pittau (OPP) (13,14) followed in this vein. Upon separation of the integrand into a standard set of basis terms, the problem could be reduced to solving for their coefficients numerically. The simple analytic extraction of triangle and bubble coefficients was the focus of the work by one of the authors (15), where the known analytic behavior of the integrand was used to straightforwardly extract the bubble and triangle coefficients. A numerical adaptation of this procedure suitable for automation was then presented in Ref. (10).

The investigation of the one-loop integral itself has also presented new directions to explore. Britto et al. (16) showed how the integral when written in a canonical form can be directly integrated. This procedure was developed further to produce new results (17) and also to provide a general analytic structure for the coefficients of one-loop amplitudes (18,19). Taking further advantage of the analytic properties of the two-particle cut amplitude, Mastrolia (20) applied Stokes' theorem and a generalized residue theorem to compute bubble coefficients via direct integration.

Extending the four-dimensional cut techniques to D dimensions (in dimensional regularization) has also provided a second very fruitful approach for the computation of the rational terms. In D dimensions the rational terms develop branch cuts and are so accessible via unitarity cuts. Giele et al. (21) elucidated

the extra structures present in D dimensions beyond those of the original four-dimensional OPP integrand. Hence they were able to compute the rational terms. Following up on this and an earlier result relating masses to D -dimensional unitarity (22), Badger presented an alternative computational approach where the $(D - 4)$ -dimensional terms are treated as an additional mass in the loop (23). A different approach advanced by Papadopoulos et al. (24) involves splitting the rational computation into two pieces. One part is computed from the one-loop integrand and is an extension to the original OPP approach, while the second part comes from a reduced form of Feynman diagrams.

These approaches have been implemented in several automated tools for the computation of one-loop amplitudes: `BlackHat` (10), `CutTools/OneLoop` (25,26), `Rocket` (27), and others (28). These programs, combined with tools for the real emission part (29,30) have yielded a host of new results at next-to-leading order (31,32,33,34,35,36).

Below we will review the main ideas of all these developments. Due to lack of space, we regret that we can neither present all details nor an exhaustive list of all results and refer the reader to the cited literature and references therein.

We begin with a review of our notation and the general structure of multi-parton scattering amplitudes and explain how to construct such amplitudes recursively at tree level. We will use the spinor formalism, and those readers unfamiliar with spinor techniques and their application to the calculation of tree-level and one-loop amplitudes may wish to consult for example Refs. (37,38,39). Section 3 discusses the use of (generalized) unitarity to construct one-loop amplitudes from tree level amplitudes, both the cut and the rational part. In Section 4 we explain how to alternatively employ a recursive approach to obtain the purely rational non-logarithmic terms of amplitudes that cannot be constructed via unitarity in four dimensions. We conclude with a summary and give an outlook on the expected progress in the near future.

2 Structure of Amplitudes

Below we briefly review our notation, which closely follows Ref. (38) (see also (37)). We then discuss the general structure of tree and one-loop amplitudes in renormalizable gauge theories to set the stage for the subsequent sections which discuss new methods for the computation of these amplitudes.

2.1 Notation and Color Decomposition

In the following we will consider amplitudes where all color¹ and coupling information has been stripped off. We can express any amplitude in terms of some basic color (and coupling) factors which are multiplied by color-ordered subam-

¹Color here and below refers to any group theory factors.

plitudes, or primitive amplitudes. These primitive amplitudes, which are defined for specific cyclic orderings of the external partons, carry all the kinematic information but no explicit color indices. The full amplitude is then assembled from the primitive amplitudes by dressing them with appropriate color factors. There exist different, but equivalent, ways of grouping the primitive amplitudes together into so-called partial amplitudes, and we refer the reader to the literature for further information, see (37, 38, 40, 41) and references therein. In what follows below, we will discuss the computation of the primitive amplitudes, concentrating on the description of the evaluation of the kinematic part. As shown recently in Ref. (42), the algorithms that we will present below can be extended to amplitudes with color information.

We express the primitive amplitudes in terms of spinor inner products,²

$$\langle j l \rangle = \langle j^- | l^+ \rangle = \bar{u}_-(k_j) u_+(k_l), \quad [j l] = \langle j^+ | l^- \rangle = \bar{u}_+(k_j) u_-(k_l), \quad (1)$$

where $u_\pm(k)$ is a massless two-component (Weyl) spinor with momentum k and positive or negative chirality, respectively, which we also write as,

$$(\lambda_i)_\alpha \equiv [u_+(k_i)]_\alpha, \quad (\tilde{\lambda}_i)_{\dot{\alpha}} \equiv [u_-(k_i)]_{\dot{\alpha}}. \quad (2)$$

Massless four-momenta can be reconstructed from the spinors by,

$$k_i^\mu (\sigma_\mu)_{\alpha\dot{\alpha}} = (\tilde{k}_i)_{\alpha\dot{\alpha}} = (\lambda_i)_\alpha (\tilde{\lambda}_i)_{\dot{\alpha}}. \quad (3)$$

Spinor products can thus be used to construct the usual momentum dot products via

$$\langle i j \rangle [j i] = \frac{1}{2} \text{Tr} [\not{k}_i \not{k}_j] = 2k_i \cdot k_j = s_{ij}. \quad (4)$$

Furthermore, we use the following notation for sums of cyclically-consecutive external momenta and their invariant masses,

$$\begin{aligned} K_{i\dots j}^\mu &\equiv k_i^\mu + k_{i+1}^\mu + \dots + k_{j-1}^\mu + k_j^\mu, \\ s_{i\dots j} &\equiv K_{i\dots j}^2, \end{aligned} \quad (5)$$

where all indices are to be understood mod n for n -particle amplitudes.

The above formalism can be extended to include massive spinors and vectors, using the well-known decomposition of any, not necessarily light-like, four-vector k into a sum of two light-like four-vectors:

$$k^\mu = k^b{}^\mu + \frac{k^2}{2k \cdot q} q^\mu. \quad (7)$$

Here q is a fixed light-like four-vector, fixing the axis of the spin for spinors, and k^b is the associated projection of the massive vector k . Massive spinors can be

²Note that we use the sign convention of most of the QCD literature, in the ‘‘twistor’’ literature a different sign convention for $[j l]$ is used, for example in Refs. (6).

constructed via

$$u_-(k, q) = \frac{1}{\langle k^b q \rangle} (\not{k} + m) |q^+\rangle = |k^{b-}\rangle + \frac{m}{\langle k^b q \rangle} |q^+\rangle, \quad (8)$$

$$u_+(k, q) = \frac{1}{[k^b q]} (\not{k} + m) |q^-\rangle = |k^{b+}\rangle + \frac{m}{[k^b q]} |q^-\rangle, \quad (9)$$

and similarly for the conjugate spinors (43). Here, the label \pm indicates that the spinors u_{\pm} are eigenstates of the projector $(1 \pm \not{s}\gamma^5)$, with the spin vector $s = k/m - m/(k \cdot q)q$. The normalization is chosen to allow a smooth limit to the massless case.

2.2 On-Shell Recursions at Tree Level

An efficient recursive technique for computing tree-level multi-parton scattering amplitudes was developed more than 20 years ago (7) and adapted for numerical implementation in various computer codes (41, 44, 45). Berends-Giele recursion connects smaller off-shell currents together to produce amplitudes. More recently it was realized that through the use of complex kinematics amplitudes can be computed entirely using only smaller on-shell amplitudes. This leads to more compact analytic expressions not only at tree level but for rational terms also at loop level. Here we briefly review the on-shell recursion relations for tree level amplitudes found and proved in Refs. (6). A recursive approach at loop level is not quite so straightforward, as we will discuss in Section 4.

At tree level, the on-shell recursion relations rely on general properties of complex functions as well as on factorization properties of scattering amplitudes. The proof (6) of the tree-level relations employs a parameter-dependent complex continuation “[j, l]”, or “shift”, of two of the external massless spinors, j and l , in an n -point process,

$$[j, l] : \quad \tilde{\lambda}_j \rightarrow \tilde{\lambda}_j - z\tilde{\lambda}_l, \quad \lambda_l \rightarrow \lambda_l + z\lambda_j. \quad (10)$$

where z is a complex number. The corresponding momenta are then continued in the complex plane as well, whereby they remain massless, $k_j^2(z) = 0 = k_l^2(z)$, and overall momentum conservation is maintained.

An on-shell amplitude containing the momenta k_j and k_l then also becomes parameter-dependent, $A(z)$. The physical amplitude is given by $A(0)$. When A is a tree amplitude or finite one-loop amplitude, $A(z)$ is a rational function of z . At tree level, $A(z)$ only has simple poles. These poles arise only from the shifted propagators of the amplitude. For example,

$$\frac{i}{K_{r\dots l\dots s}^2} \rightarrow \frac{i}{K_{r\dots s}^2 + z \langle j^- | \not{K}_{r\dots s} | l^- \rangle}, \quad (11)$$

if the set of legs $\{r, \dots, s\}$ contains leg l , which is shifted according to eq. (10). In the vicinity of the location of the pole z_{rs} , the complex continued amplitude

is then schematically given by,

$$\lim_{z \rightarrow z_{rs}} A(z) = \sum_h A_L^h(z) \frac{i}{K_{r\dots s}^2 + z \langle j^- | \not{K}_{r\dots s} | l^- \rangle} A_R^{-h}(z), \quad (12)$$

where $h = \pm 1$ labels the helicity of the intermediate state, and the labels L and R denote amplitudes with fewer legs, which the propagator eq. (11) connects. The number of poles z_{rs} in the complex plane is given by the number of ways the set of external legs can be partitioned such that the legs j and l always appear on opposite sides of the z -dependent propagator.

We can now use Cauchy's theorem,

$$\frac{1}{2\pi i} \oint_C \frac{dz}{z} A(z) = 0, \quad (13)$$

where the contour C is taken around the circle at infinity, and the integral vanishes if the complex continued amplitude $A(z)$ vanishes as $z \rightarrow \infty$. Evaluating the integral as a sum of residues, we can then solve for the physical amplitude $A(0)$ to obtain,

$$A(0) = - \sum_{\text{poles } \alpha} \text{Res}_{z=z_\alpha} \frac{A(z)}{z} = \sum_{r,s} \sum_h A_L^h(z = z_{rs}) \frac{i}{K_{r\dots s}^2} A_R^{-h}(z = z_{rs}). \quad (14)$$

The on-shell amplitudes with fewer legs, A_L and A_R , are evaluated in kinematics that have been shifted by eq. (10) with $z = z_{rs}$, where eq. (11) has a pole,

$$z_{rs} = - \frac{K_{r\dots s}^2}{\langle j^- | \not{K}_{r\dots s} | l^- \rangle}. \quad (15)$$

In the following, such shifted, on-shell momenta will be denoted by $k(z = z_{rs}) \equiv \hat{k}$. A typical contribution to the sums in eq. (14) is illustrated in Fig. 1.

We have thus succeeded in expressing the n -point amplitude A in terms of sums over on-shell, but complex continued, amplitudes with fewer legs, which are connected by scalar propagators. These recursion relations can be extended to massive QCD and other theories (46, 47). Moreover, for certain helicity configurations, this recursion relation can be solved explicitly, leading to new all-multiplicity expressions for these amplitudes (48).

The basic ingredients to obtain such a recursion relation are complex momenta and analysis, which are necessary to make 3-point vertices non-vanishing; factorizability, which is responsible for the simple pole structure; and the vanishing of the boundary contribution as $z \rightarrow \infty$. At tree level in QCD, one can always find complex continuations where this boundary condition vanishes. However, as we will see in Section 4 below, this is not the case at the one-loop level, and a recursive approach becomes considerably more complicated. Other theories such as a scalar ϕ^4 theory have non-vanishing $z \rightarrow \infty$ behavior already at the tree level, which spoils the recursive approach. Studies of the origin of these boundary terms and their relation to the Lagrangian can be found in Refs. (49). Furthermore, additional amplitude structures related to on-shell recursion relations and twistor space have been uncovered (50).

2.3 Structure of One-Loop Amplitudes

We now turn to the discussion of gauge-theory one-loop amplitudes, the main subject of this review. From here on, we will denote one-loop amplitudes explicitly with a superscript $A^{1\text{-loop}}$, and tree amplitudes without superscript simply by A .

Using reduction techniques (51, 52, 53) any m -point scalar integral, $m > 4$, can be reduced to scalar integrals with at most four propagators. That is, any one-loop n -point amplitude $A_n^{1\text{-loop}}$ can be decomposed into a basis B_4 of scalar box, triangle, bubble and tadpole integrals, with rational coefficients in four dimensions. In D dimensions, for example when working in dimensional regularization where $D = 4 - 2\varepsilon$, then the basis B_D is extended to include a scalar pentagon. The coefficients of the D -dimensional basis scalar integrals can be decomposed into purely four-dimensional coefficients after expanding in ε . Purely rational terms are generated when terms higher order in ε in the coefficients are multiplied by the poles in the integrals,

$$A_n^{1\text{-loop}} = \sum_{j \in B_D} c_j^D \mathcal{I}_j^D = \sum_{j \in B_4} c_j^{D=4} \mathcal{I}_j^D + \mathcal{R}_n. \quad (16)$$

Illustrative examples of integrals of the basis B are shown in Fig. 2.

We will see in the next two sections how to obtain these coefficients and rational terms in efficient ways. The scalar integrals contain infrared and ultraviolet divergences that are regulated via dimensional regularization, and depend logarithmically or polylogarithmically on momentum-invariants. The integrals appearing in eq. (16) are known and tabulated for example in Refs. (4, 54). In order to compute one-loop matrix elements the task is therefore reduced to the determination of the coefficients, it is not necessary to perform any integrals.

For amplitudes with only massless particles, the tadpoles vanish. In $\mathcal{N} = 4$ supersymmetric theories, as counting of powers of loop momenta in one-loop integrals reveals, only box integrals contribute with ($D = 4$)-dimensional coefficients (i. e. free of ε terms), and in $\mathcal{N} = 1$ supersymmetry bubble, triangle, and box integrals contribute, with four-dimensional coefficients (4). That is, theories with unbroken supersymmetries do not contain purely rational terms that are not associated with any of the integrals in the basis. One-loop supersymmetric amplitudes can therefore be completely reconstructed from unitarity cuts, as we will now discuss.

3 Extraction of Integral Coefficients via Unitarity

The problem of computing eq. (16) has been reduced to determining the coefficients, c_j , multiplying the known basis integral functions, in the most efficient manner possible. The nature of eq. (16) suggests the use of unitarity cuts to isolate particular integral coefficients. At the most basic level a unitary cut effectively replaces a propagator with an on-shell delta function, i.e. we “cut” the

propagator with the replacement,

$$\frac{1}{p^2 - m^2 + i\epsilon} \rightarrow \delta^{(+)}(p^2 - m^2). \quad (17)$$

In the original unitarity approach (4) only two propagators were cut but more recent developments have highlighted the benefits of applying multiple cuts (5, 12). The application of multiple cuts is known as Generalized Unitarity and has become the foundation of the most recent developments in the literature.

Our starting point is the form of eq. (16) decomposed in the B_4 basis, we postpone the discussion of the general D -dimensional case using B_D to Section 3.3. The purely rational terms are independent of any possible cuts in four dimensions and therefore only the remaining “cut-constructible” pieces are accessible via a unitarity technique.

We apply a number of cuts to the expression of the one-loop amplitude and match this expression to that of the basis decomposition, eq. (16), with the same set of cuts applied. This allows us to directly relate the cut expression to the basis integral coefficients. This procedure is repeated with as many different sets of cuts as is needed to compute all the basis coefficients. Rather than actually applying the cuts to the full expression for the one loop amplitude, computed for example with Feynman diagrams, we construct the cut expression simply by multiplying appropriate on-shell tree amplitudes together. This allows us to take advantage of efficient, compact forms of tree amplitudes produced via recursion relations, for example those of Section 2.2.

Below, we describe two unitarity approaches for the extraction of integral coefficients. They both utilize knowledge of the *integrand*, $\tilde{A}(l)$, of the one-loop amplitude, $A_n^{1\text{-loop}} = \int dl \tilde{A}_n(l)$, to derive the basis integral coefficients. The first, described in Section 3.1, is based upon the examination of the behavior of the loop integrand and the loop momenta in the complex plane. The second, described in Section 3.2, known as the Ossola, Papadopoulos and Pittau (OPP) method, relies upon computing the coefficients of the general structure of the loop integrand itself.

3.1 Generalized Unitarity in Four Dimensions

In general we want to isolate as few basis integral coefficients as possible with each cut that we consider. It is easy to see that a quadruple cut can be used to isolate, on the basis side, a single box coefficient. There are not enough propagators in the bubble and triangle integrals to accommodate so many cuts. The set of cuts we require to compute all box coefficients corresponds simply to all possible boxes that could be present.

3.1.1 BOXES A very straightforward way to extract a specific box coefficient from a quadruple cut expression was proposed by Britto et al. in (12). The momentum circulating inside a loop without cuts is off-shell and can therefore

be parametrized in terms of four free components. Applying a cut to one of the propagators in the expression of the one-loop amplitude reduces the number of free components in this loop momentum by one. Second, third and fourth cuts will then reduce the number of free components to zero. The loop momentum for the box is then completely frozen by the four delta-function constraints. The desired scalar box coefficient can now be read off from the resulting rational expression,

$$\int \frac{d^4 l}{(2\pi)^4} \frac{d(l)}{(l^2 + i\epsilon)(l_1^2 + i\epsilon)(l_2^2 + i\epsilon)(l_3^2 + i\epsilon)} \Big|_{l_i^2 + i\epsilon \rightarrow \delta^+(l_i^2)} \longrightarrow \frac{1}{2} \sum_{\text{solutions}} d(l_{\text{solution}}). \quad (18)$$

The coefficient is a product of four tree amplitudes that sit at the four corners of the cut box as illustrated in Fig. 3. The momenta flowing into the trees satisfy the four cut constraints. In general there are two possible solutions to the constraints parameterizing the box. For example with at least one massless leg (leg 1) we have (10, 55),

$$l_{\pm}^{\mu} = \frac{\langle 1^{\mp} | \not{K}_2 \not{K}_3 \not{K}_4 \gamma^{\mu} | 1^{\pm} \rangle}{2 \langle 1^{\mp} | \not{K}_2 \not{K}_4 | 1^{\pm} \rangle}. \quad (19)$$

Inserting each solution into the product of four trees at each corner and then summing the two results gives the complete box coefficient,

$$d_0 = \frac{1}{2} \sum_{a=\pm} d_a, \quad d_a = A_1(l_a) A_2(l_a) A_3(l_a) A_4(l_a). \quad (20)$$

Further discussion on the use of both solutions and alternative approaches can be found in (56).

3.1.2 TRIANGLES To compute triangle coefficients, we first apply a triple cut to our one-loop amplitude. Unlike the box case, this cut isolates not just a single triangle but also any boxes which also contain the same triple cut. Furthermore we are left with a loop integral with a single free component. Our cut expression therefore still depends upon the loop integration. To extract the triangle coefficient isolated by the triple cut therefore requires two steps. First, we must remove the boxes polluting the triple cut expression. Then we must relate the triangle integral, which depends upon the remaining free loop-parameter, to the scalar triangle basis integral.

As was first proposed in (15), both issues can be solved simultaneously by examining the analytic behavior of the triple cut expression in the free parameter t of the loop momentum. We choose the following specific parametrization of the loop momentum,

$$l^{\mu} = K_1^{b,\mu} + K_2^{b,\mu} + \frac{t}{2} \langle K_1^{b,-} | \gamma^{\mu} | K_2^{b,-} \rangle + \frac{1}{2t} \langle K_2^{b,-} | \gamma^{\mu} | K_1^{b,-} \rangle. \quad (21)$$

The massless momenta $K_i^{b,\mu}$ are given by

$$K_1^{b,\mu} = \gamma \alpha \frac{\gamma K_1^{\mu} + S_1 K_2^{\mu}}{\gamma^2 - S_1 S_2}, \quad K_2^{b,\mu} = -\gamma \alpha' \frac{\gamma K_2^{\mu} + S_2 K_1^{\mu}}{\gamma^2 - S_1 S_2},$$

$$\begin{aligned} \gamma_{\pm} &= -(K_1 \cdot K_2) \pm \sqrt{\Delta}, & \Delta &= -\det(K_i \cdot K_j) = (K_1 \cdot K_2)^2 - K_1^2 K_2^2, \\ \alpha &= \frac{S_2(S_1 - \gamma)}{(S_1 S_2 - \gamma^2)}, & \alpha' &= \frac{S_1(S_2 - \gamma)}{(S_1 S_2 - \gamma^2)}, \end{aligned} \quad (22)$$

with $S_i = K_i^2$.

By definition, any box terms containing our chosen triple cut will also contain an additional propagator, $1/(l - K_4)^2$. Inserting the parametrization for l^μ of eq. (21) into this additional propagator leads to the development of two poles, t_{\pm} , in the propagator $(l - K_4)^2 \propto (1/t)(t - t_-)(t - t_+)$. We can take advantage of the occurrence of these poles to separate the box terms from the triangle pieces.

The numerators of these box poles are given by an effective quadruple cut generated by the extra pole along with the original triple-cut. As we have seen above, the quadruple cut of a box actually corresponds to one of the two contributions in the construction of a box coefficient. Therefore each box term can be written as a sum of two residue terms, $\sum_{i=\pm} d_i/(\chi_i(t - t_i))$, with d_i the residue corresponding to the box coefficient of the pole t_i and χ_i a constant factor depending upon the box in question.

Analytically, in order to remove these box terms we simply expand the parametrized triple cut integrand expression around $t \rightarrow \infty$. The box terms behave as $1/t \rightarrow 0$ in this limit and thus drop out. Taking a parameter to infinity numerically is problematic, so instead we use a different approach in the computer code `BlackHat` (10). Considering t as a complex parameter, the box terms appear as poles in the complex plane of t , whereas the triangle coefficient is at the origin of the t plane. To remove the box terms we simply systematically “clean” the complex plane by subtracting all box pole terms from our triple cut expression. A final complication to both numerical and analytic approaches is the presence of the $1/t$ factor in the box propagator. To account for this we add back the sum of all box terms evaluated at $t = 0$, i.e. add $(d_- - d_+)/(\chi_i(t_- - t_+))$ for each box term. An alternative approach to this last step and further discussion on the analytic properties of the three-mass triangle can be found in (15) and (57). In addition, the application of on-shell recursion to the computation of certain triangle coefficients can be found in (58).

After the elimination of box terms we are left with a finite power series in t ,

$$C(t) \equiv A_1(t)A_2(t)A_3(t) - \sum_{i=\pm} \frac{d_i}{\chi_i(t - t_i)} = \sum_{j=-n}^n c_j \int dt t^j, \quad (23)$$

where the c_j are rational coefficients. The upper and lower limits $\pm n$ of the sum is determined by the theory in question, for example $n = 3$ for renormalizable theories. To relate this sum of terms to the scalar triangle integral we first note that, for this particular parametrization, the integrals over any power of t in eq. (23) vanish as proved in (15). Then the only remaining term, $c_0 \int dt$, is in the form of a rational coefficient multiplying a scalar triangle integral. In an analytic formalism the series expansion around $t \rightarrow \infty$ will automatically isolate this term.

So we can directly relate this sole remaining term to the desired coefficient of the basis triangle integral we have isolated with our triple cut. Numerically, our final step is to note that, since the power series in t terminates at a finite power, n , the full contour integral is equivalent to a discrete Fourier projection (10) with $2n + 1$ evaluation points. The triangle coefficient is therefore given by,

$$c_0 = \frac{1}{2n + 1} \sum_{j=-n}^n C \left(t_0 e^{2\pi i j / (2n+1)} \right). \quad (24)$$

The arbitrary complex number t_0 is the radius of the numerical Fourier projection, as illustrated in Fig. 4. For technical details we refer to Ref. (10).

3.1.3 BUBBLES The computation of bubble coefficients proceeds along similar lines as above. A two-particle cut isolates a single bubble coefficient, but will also capture triangles and boxes which share the same cut. Again we use the differing analytic properties of the terms with additional propagators to separate the triangle and box terms from the bubble coefficient.

As before, we start from a specially chosen parametrization of the loop momentum. A two-particle cut leaves two free parameters, y and z . We then choose to parametrize the two-particle cut, bubble, loop-momenta as,

$$l_i^\mu(y, z) = \frac{1}{2} K_i^\mu + (y - \frac{1}{2}) \left(\tilde{K}_1^\mu - \chi^\mu \right) + \frac{z}{2} \langle \tilde{K}_1^- | \gamma^\mu | \chi^- \rangle + \frac{y(1-y)}{2z} \langle \chi^- | \gamma^\mu | \tilde{K}_1^- \rangle. \quad (25)$$

Here χ , an arbitrary massless momentum, is used to define the massless momentum $\tilde{K}_1^\mu = K_1^\mu - \chi^\mu$, with its normalization chosen so that $K_1 \cdot \chi = K_1^2/2$.

The triangle and box terms sharing the two-particle cut will contain at least one additional propagator $1/(l - K_2)^2$. The parametrization of eq. (25) will then introduce poles in y or z . The residue of the poles in terms of y is given by, effectively, a triple cut expression, which is a combination of the pole and the original two-particle cut. Contained inside this expression are a single triangle, isolated by the effective triple cut, and possibly box terms with the same cut.

Unfortunately, the more complicated structure of the momentum parametrization and the bubble integrand means that a simple extension of the triangle procedure is not so straightforward. This is because for the parametrization (25) the integrals over positive powers of y are non-zero, and given by,

$$\int dy y^n = \frac{1}{n+1} \int dy. \quad (26)$$

The integrals over powers of z still vanish. We must therefore alter our approach for extracting the bubble coefficient. As before, we discard any terms in the expansion around $z \rightarrow \infty$ that depend upon z , but we must retain the coefficients of all powers of y (which are all guaranteed to be positive due to our parametrization choice). For a renormalizable theory the maximum power is y^2 . We can relate

these terms to the scalar integral using eq. (26), which is independent of y and z , $\int dydz$. The sum of the resulting terms forms *only* part of the bubble coefficient.

The source of the remaining contribution is the triangle expression from the residues of the poles in z . This effective triple cut does not vanish in the double expansion in y and z . Therefore, we obtain an additional contribution which needs to be subtracted from the part of the bubble coefficient computed in the previous paragraph. Further details on this subtraction term can be found in Ref. (15).

To numerically extract the bubble coefficient we must first “clean” the complex plane of all pole terms. Computing the residues of each pole involves simply computing the triple cut at the location of each pole. Once all pole terms have been removed we are free to extract the bubble coefficient from the remaining non-pole terms using a double discrete Fourier projection, in both y and z . Instead of naively evaluating at as many points as there are coefficients in y and z we use the nature of our parametrization to reduce the number of points at which we need to evaluate z by one. The coefficient in a renormalizable theory is given by

$$b_0 = \frac{1}{20} \sum_{j=0}^4 \left[B(y=0, z=t_0 e^{2\pi i j/5}) + 3B(y=2/3, z=t_0 e^{2\pi i j/5}) \right]. \quad (27)$$

$B(y, z)$ denotes the two-particle cut from which triangles and boxes have been subtracted that share this cut. The more general case is given in (10). Alternative approaches to the computation of the bubble coefficients have been proposed in the literature, such as Mastrolia’s use of Stokes Theorem (20).

3.1.4 MASSIVE PARTICLES The expressions we have given above are for amplitudes with purely massless particles. The addition of massive particles which do not circulate in the loop is straightforwardly accommodated within the above, with no changes. Including massive particles inside the circulating loop requires further exposition. Two changes are required, firstly the loop momentum parametrization needs to be extended to include massive particles. Secondly we must also compute the coefficients of tadpole integrals in addition to the bubbles, triangles and boxes. A detailed discussion of the extension of the procedure to the computation of massive particles as well as the computation of the tadpole terms themselves is given in (59). In addition there is the problem of the wave-function renormalization with massive particles, which has been addressed in Ref. (60).

3.2 Extraction of Integral Coefficients at the Integrand Level

So far we have described methods which used analytic limits or a combination of the subtraction of poles on the complex plane and discrete Fourier projections. An alternative approach developed by Ossola, Papadopoulos and Pittau (OPP) uses the knowledge of the general structure of the integrand $\tilde{A}(l)$ instead. The integrand is built up from a standard set of terms. These terms either vanish

upon integration or correspond to one of the scalar integral basis functions of eq. (16). Computing the scalar basis integral coefficients then reduces to the problem of finding the coefficients of the OPP decomposition of the integrand.

In four dimensions, the integrand can be written as,

$$\begin{aligned} \tilde{A}_n(l) = & \sum_{1 \leq i_1 < i_2 < i_3 < i_4 \leq n} \frac{d_{i_1 i_2 i_3 i_4}(l)}{D_{i_1} D_{i_2} D_{i_3} D_{i_4}} + \sum_{1 \leq i_1 < i_2 < i_3 \leq n} \frac{c_{i_1 i_2 i_3}(l)}{D_{i_1} D_{i_2} D_{i_3}} \\ & + \sum_{1 \leq i_1 < i_2 \leq n} \frac{b_{i_1 i_2}(l)}{D_{i_1} D_{i_2}} + \sum_{1 \leq i_1 \leq n} \frac{a_{i_1}(l)}{D_{i_1}}, \end{aligned} \quad (28)$$

with the propagator $D_i = (l - K_i)^2 - m_i^2$, where the mass of the cut propagator with momentum l_i has mass m_i . From now on we include massive particles in the discussion. The form of the numerators in eq. (28) depend upon the basis we choose for the loop momenta. We wish to choose this momentum basis so that each scalar integral basis coefficient of B_4 corresponds to a single term in the integrand decomposition and the integrals over the remaining structures vanish. In the form originally presented by OPP (13), a momentum parametrization for the box, triangle and bubble very similar to eqs. (19), (21) and (25) was used.

An alternative momentum parametrization, presented by Ellis et al. (61), is related to the van Neerven-Vermaseren basis (52). The generic form of a momentum in this basis is

$$l^\mu = \sum_{j=1}^{D_P} v_j^\mu + \sum_{j=1}^{D_T} \alpha_j n_j^\mu. \quad (29)$$

This is a decomposition into two sets of basis vectors. The vectors v_j^μ span the physical space defined by the external legs K_i and the vectors n_j^μ span the space transverse to this physical space. For a box $D_T = 1$ and $D_P = 3$, for a triangle $D_T = 2$ and $D_P = 2$ and for a bubble $D_T = 3$ and $D_P = 1$. The basis vectors are chosen such that $n_i \cdot n_j = \delta_{ij}$, $n_i \cdot K_j = 0$ and $n_i \cdot v_j = 0$. The v_j 's are chosen such that any cut legs are on-shell.

The numerators of the propagator terms are then arranged in the following way (61),

$$d_{i_1 i_2 i_3 i_4}(l) = c_{i_1 i_2 i_3 i_4}^0 + c_{i_1 i_2 i_3 i_4}^1 t_1, \quad (30)$$

$$\begin{aligned} c_{i_1 i_2 i_3}(l) = & c_{i_1 i_2 i_3}^0 + c_{i_1 i_2 i_3}^1 t_1 + c_{i_1 i_2 i_3}^2 t_2 + c_{i_1 i_2 i_3}^3 (t_1^2 - t_2^2) \\ & + t_1 t_2 (c_{i_1 i_2 i_3}^4 + c_{i_1 i_2 i_3}^5 t_1 + c_{i_1 i_2 i_3}^6 t_2), \end{aligned} \quad (31)$$

$$\begin{aligned} b_{i_1 i_2}(l) = & c_{i_1 i_2}^0 + c_{i_1 i_2}^1 t_1 + c_{i_1 i_2}^2 t_2 + c_{i_1 i_2}^3 t_3 + c_{i_1 i_2}^4 (t_1^2 - t_3^2) \\ & + c_{i_1 i_2}^5 (t_2^2 - t_3^2) + c_{i_1 i_2}^6 t_1 t_2 + c_{i_1 i_2}^7 t_1 t_3 + c_{i_1 i_2}^8 t_2 t_3. \end{aligned} \quad (32)$$

$$a_{i_1}(l) = c_{i_1}^0 + c_{i_1}^1 t_1 + c_{i_1}^2 t_2 + c_{i_1}^3 t_3 + c_{i_1}^4 t_4, \quad (33)$$

for the tadpole, bubble, triangle and box, $i = 1, 2, 3, 4$ respectively. Here the $t_j = (n_j \cdot l)$ depend on the specific parametrization of the loop momentum, which

is chosen differently for boxes, triangles, bubbles and tadpoles. The coefficients we wish to compute are the c^0 terms which correspond to the scalar basis integral coefficients. We will not discuss the computation of the tadpole terms here, methods to compute these can be found in (13, 19, 59, 60, 61). The remaining coefficients multiply t_j terms (or combinations of such terms), which vanish upon integration over l . As in section 3.1, the choice of the representation for the loop momentum is crucial in this approach.

Trying to solve for the entire set of coefficients at once is clearly not the optimal approach. Using unitarity cuts we can isolate individual terms of the integrand. The application of all possible cuts allows us to systematically solve for all of the coefficients sequentially. Isolating a single box term $d_{i_1 i_2 i_3 i_4}$ with a quadruple cut works in the same way as in section 3.1. Again we have two solutions for the completely frozen box loop momentum. For the momentum basis corresponding to the integrand decomposition eq. (30) these are

$$l_{\pm}^{\mu} = v_1^{\mu} + v_2^{\mu} + v_3^{\mu} \pm \sqrt{m_0^2 - (v_1 + v_2 + v_3)^2} n_1^{\mu}. \quad (34)$$

As above, the box coefficients in the OPP basis are given by products of four tree amplitudes,

$$c_{i_1 i_2 i_3 i_4}^0 = \frac{1}{2} \sum_{a=\pm} d_a, \quad d_a = A_1(l_a) A_2(l_a) A_3(l_a) A_4(l_a), \quad (35)$$

$$c_{i_1 i_2 i_3 i_4}^1 = \frac{1}{2} (d_+ - d_-).$$

Here, $c_{i_1 i_2 i_3 i_4}^0$ is the desired scalar box integral coefficient, d_0 (cf. eq. (20)). The other coefficient is needed for the computation of the triangle coefficients.

For the computation of the triangle coefficients we apply a triple cut to isolate the particular triangle we are interested in. Much like before this means that we also have box terms polluting the result. To solve this problem we subtract the complete box contribution from the integrand. So in order to find the triangle coefficients $c_{i_1 i_2 i_3}^k$ we do not evaluate $A_1(l) A_2(l) A_3(l)$, but instead,

$$A_1(l) A_2(l) A_3(l) - \sum_{i_4} \frac{d_{i_1 i_2 i_3 i_4}(l)}{D_{i_4}}, \quad (36)$$

at different choices for the loop momentum of the triangle. This is in contrast to the procedure of the previous section. There we subtracted the residue of the box pole from the triangle rather than the entire contribution of the box (20) from the integrand as above. The triangle momentum parametrization corresponding to the integrand structure eq. (31) contains one free parameter which we label α ,

$$l^{\mu} = v_1^{\mu} + v_2^{\mu} + \sqrt{m_0^2 - \alpha^2 - (v_1 + v_2)^2} n_1^{\mu} + \alpha n_2^{\mu}. \quad (37)$$

There are seven unknown coefficients in eq. (31), so we need to evaluate this at seven, in principle arbitrary, values of α to determine all coefficients. For

increased numerical stability, however, they can be chosen to lie on a circle as in the previous section. The resulting set of linear equations can then be solved to find the full set of coefficients, which is needed in the computation of the bubble coefficient.

Finally, in order to compute the bubbles we apply a double cut, which again isolates a single bubble but also any triangle and box coefficients that share the same cut. Again we simply subtract the unwanted terms from the integrand to remove them. To find the coefficients $b_{i_1 i_2}^k$ we evaluate

$$A_1(l)A_2(l) - \sum_{i_3} \frac{c_{i_1 i_2 i_3}(l)}{D_{i_3}} - \frac{1}{2!} \sum_{i_3 i_4} \frac{d_{i_1 i_2 i_3 i_4}(l)}{D_{i_3} D_{i_4}}, \quad (38)$$

at different values of the loop momentum of the bubble. Here the bubble loop momentum corresponding to the parametrization eq. (32) is,

$$l^\mu = v_1^\mu + \sqrt{m_0^2 - \alpha_1^2 - \alpha_2^2 - v_1^2} n_1^\mu + \alpha_1 n_2^\mu + \alpha_2 n_3^\mu, \quad (39)$$

with two free parameters, α_1 and α_2 . Solving for the nine coefficients in eq. (32) requires nine linear equations. These can be generated by choosing nine different values of l via the choice of the two free parameters. The full set of nine coefficients is only required if we wish to compute the tadpole coefficients, which only appear if massive particles are present in the loop. Further details can be found in Refs. (60, 61).

3.3 Rational Terms from D-Dimensional Generalized Unitarity

We have so far restricted ourselves to working with cut legs in four dimensions, keeping the rational terms out of reach. Considering cuts in D dimensions allows us to use the B_D integral basis of eq. (16), bringing the computation of all terms within our grasp. This is related to van Neerven's important observation that dispersion relations for Feynman integrals converge in dimensional regularization (62). There are multiple different approaches to go beyond four-dimensional cuts as already proposed in Refs. (22). The additional $D - 4$ components can be related to massive terms in four dimensions (22). In a related approach the $D - 4$ components can be converted to an additional integral which can be used to compute the full amplitude (63).

Alternatively, we can directly extend the approaches of either Section 3.1 or Section 3.2, as we will now describe, starting with the generalization of Section 3.2.

3.3.1 D-DIMENSIONAL UNITARITY AT THE INTEGRAND LEVEL OPP have suggested a two-step computational procedure. Here, the $D - 4$ terms in the numerator of the integrand are computed using a separate set of Feynman diagrams. The corresponding Feynman rules have been derived for QCD and electroweak

theories in a series of papers (24, 64). The $D - 4$ contributions from the denominator of the integrand are found by computing coefficients of an extended OPP basis structure for the integrand (13, 24).

A direct extension of the OPP approach to D dimensions was derived by Giele et al. (21). This approach combines trees in higher dimensions with an extended integrand basis for the one-loop integrand, taking into account the additional structure in higher dimensions. Again as in Section 3.2 the choice of the loop momentum determines the form of the integrand structures. The form of the higher dimensional loop momenta can be decomposed into a four-dimensional part \vec{l} and an orthogonal $(D - 4)$ -dimensional part \tilde{l} , $l^\mu = \vec{l}^\mu + \tilde{l}^\mu$. The on-shell constraint then means that $l^2 = \vec{l}^2 + \tilde{l}^2$ and so the four-dimensional component effectively becomes massive with mass $-\tilde{l}^2 = \mu^2$, where μ^2 is the ‘‘scale’’ of the higher-dimensional subspace.

Since the external momenta remain in four dimensions, we find that there are a limited number of additional integrand structures that can be present because the external momenta are orthogonal to the $D - 4$ additional transverse dimensions. The numerator structures can only depend upon the higher-dimensional terms through even powers of μ . Similarly, there can be at most one additional cut leg, since μ^2 is fixed by the fifth constraint. Therefore we must include a pentagon in the integrand basis and so for a renormalizable theory the extended integrand structures are given by,

$$\begin{aligned} \tilde{A}_n(l) = & \sum_{1 \leq i_1 < i_2 < i_3 < i_4 < i_5 \leq n} \frac{\tilde{e}_{i_1 i_2 i_3 i_4 i_5}(l)}{D_{i_1} D_{i_2} D_{i_3} D_{i_4} D_{i_5}} + \sum_{1 \leq i_1 < i_2 < i_3 < i_4 \leq n} \frac{\tilde{d}_{i_1 i_2 i_3 i_4}(l)}{D_{i_1} D_{i_2} D_{i_3} D_{i_4}} \\ & + \sum_{1 \leq i_1 < i_2 < i_3 \leq n} \frac{\tilde{c}_{i_1 i_2 i_3}(l)}{D_{i_1} D_{i_2} D_{i_3}} + \sum_{1 \leq i_1 < i_2 \leq n} \frac{\tilde{b}_{i_1 i_2}(l)}{D_{i_1} D_{i_2}} + \sum_{1 \leq i_1 \leq n} \frac{\tilde{a}_{i_1}(l)}{D_{i_1}}. \end{aligned} \quad (40)$$

Here the numerator coefficients are given by,

$$\begin{aligned} \tilde{e}_{i_1 i_2 i_3 i_4 i_5}(l) &= c_{i_1 i_2 i_3 i_4 i_5}^0, \\ \tilde{d}_{i_1 i_2 i_3 i_4}(l) &= d_{i_1 i_2 i_3 i_4}(\vec{l}) + \mu^2 (c_{i_1 i_2 i_3 i_4}^2 + t_1 c_{i_1 i_2 i_3 i_4}^3) + \mu^4 c_{i_1 i_2 i_3 i_4}^4, \\ \tilde{c}_{i_1 i_2 i_3}(l) &= c_{i_1 i_2 i_3}(\vec{l}) + \mu^2 (t_1 c_{i_1 i_2 i_3}^8 + t_2 c_{i_1 i_2 i_3}^9 + c_{i_1 i_2 i_3}^{10}), \\ \tilde{b}_{i_1 i_2}(l) &= b_{i_1 i_2}(\vec{l}) + \mu^2 c_{i_1 i_2}^{10}, \\ \tilde{a}_{i_1}(l) &= a_{i_1}(\vec{l}). \end{aligned} \quad (41)$$

where again $t_j = n_j \cdot l$.

The attentive reader may be worried about how this basis can be used if we have a fractional number of additional dimensions, for example when $D = 4 - 2\varepsilon$. This problem can be sidestepped by noting that the dependence of the amplitudes upon the $(D - 4)$ -dimensional subspace is *linear*. So the fractional dimensional structure of the amplitude can be reconstructed by evaluating the amplitude at two different integer dimensions. Using $A_D^{1\text{-loop}} = A_0^{1\text{-loop}} + (D - 4)A_1^{1\text{-loop}}$ the full D -dimensional amplitude can then be reconstructed (21). This allows us to

freely choose the exact form of the regularization scheme. The integer dimension chosen when evaluating the trees that enter the calculations is arbitrary up to the constraint that the dimension has to be an even number if fermions are present in the loop.

The final step is to relate the new integrand structures of eq. (41), proportional to powers of μ , to their contribution in eq. (16). As before, terms proportional to t_j terms will vanish and so we are left with terms proportional only to μ . Scalar integrals multiplied by powers of μ can be related to scalar integrals in higher dimensions. From eq. (41) we have the following different integrals,

$$\begin{aligned}
\int d^D l \frac{\mu^2}{D_{i_1} D_{i_2} D_{i_3} D_{i_4}} &= -\frac{D-4}{2} I_{i_1 i_2 i_3 i_4}^{D+2} \xrightarrow{D \rightarrow 4} 0 \\
\int d^D l \frac{\mu^4}{D_{i_1} D_{i_2} D_{i_3} D_{i_4}} &= \frac{(D-4)(D-2)}{4} I_{i_1 i_2 i_3 i_4}^{D+4} \xrightarrow{D \rightarrow 4} -\frac{1}{6} \\
\int d^D l \frac{\mu^2}{D_{i_1} D_{i_2} D_{i_3}} &= -\frac{(D-4)}{2} I_{i_1 i_2 i_3}^{D+2} \xrightarrow{D \rightarrow 4} -\frac{1}{2} \\
\int d^D l \frac{\mu^2}{D_{i_1} D_{i_2}} &= -\frac{(D-4)}{2} I_{i_1 i_2}^{D+2} \xrightarrow{D \rightarrow 4} \frac{m_{i_1}^2 + m_{i_2}^2}{2} - \frac{1}{6} S_{i_1 i_2}. \quad (42)
\end{aligned}$$

where $S_{i_1 i_2}$ is the mass of the bubble labelled by i_1 and i_2 . Examining the limits of these integrals as we return to four dimensions, we see that the integrals are finite and correspond to purely rational numbers. Each new integrand factor therefore contributes to the rational term.

Computing the one-loop amplitude is now very similar to the cut-computation procedure of Section 3.2. Starting with the pentagon we find that the loop momenta will be completely frozen by the four cuts on the four-dimensional component of l_5^μ and the constraint on $\mu^2 = -\tilde{l}^2$ from the fifth propagator $(\tilde{l} + \tilde{l} - K_5)^2 = m_5^2$. The resulting expression is then inserted into the penta-cut so that we find the pentagon coefficient using,

$$c_{i_1 i_2 i_3 i_4 i_5}^0 = A_1(l) A_2(l) A_3(l) A_4(l) A_5(l). \quad (43)$$

The trees must be evaluated, as described above, at two different integer dimension choices for the internal loop momentum. The pentagon coefficient is proportional to $D-4$ and so will vanish in the four-dimensional limit. We need it only for subtraction when computing the box terms as we will now explain.

The box is computed as before but with the pentagon subtracted,

$$A_1(l) A_2(l) A_3(l) A_4(l) - \sum_{i_5} \frac{e_{i_1 i_2 i_3 i_4 i_5}(l)}{D_{i_5}}. \quad (44)$$

With three additional coefficients to be determined, compared to the four-dimensional case, we need three additional evaluation points in order to generate enough equations to solve for all coefficients. All coefficients are required for the computation of the triangle terms. Computing the triangle and bubble contributions

to the rational terms follows in a similar vein as for the boxes and we direct the reader to Ref. (21) for further details on the computation of all such contributions.

3.3.2 FOUR-DIMENSIONAL GENERALIZED UNITARITY WITH A $D - 4$ -DIMENSIONAL MASS The differing dependence of the rational terms of eq. (41) on μ^2 suggests that we could use the analytic structure of the integrand to compute the rational terms at the integral level. This approach of Badger (23) is similar in spirit to the extraction of the cut-coefficients described in Section 3.1. Here the loop momentum is massive and four-dimensional rather than massless and D -dimensional.

To compute the rational contribution of the box, we start from the quadruple cut expression of a box. Now each cut leg has an additional mass μ^2 . This cut isolates a single box coefficient and also any pentagon terms which share the same cut. Schematically we have,

$$A_1(l(\mu^2))A_2(l(\mu^2))A_3(l(\mu^2))A_4(l(\mu^2)) = r_1 + r_2\mu^2 + r_3\mu^4 + \sum_i \frac{e_i^0}{\chi_i(\mu^2 - \mu_i^2)}. \quad (45)$$

where μ_i^2 is the pole in μ^2 for the pentagon i , χ_i is a constant factor depending on the pentagon in question. The additional propagator of the pentagon terms shows up as a $1/(\mu^2 - \mu_i^2)$ factor. We wish to separate these terms as well as the other terms in the powers series in μ^2 from each other. Here we only want the coefficient r_3 of μ^4 , which is the term that contributes to the purely rational part, cf. eq. (42). So simply expanding $A_1(l(\mu^2))A_2(l(\mu^2))A_3(l(\mu^2))A_4(l(\mu^2))/\mu^4$ around the limit $\mu^2 \rightarrow \infty$ will give us the coefficient directly.

Moving on, performing a triple cut isolates a single triangle as well as boxes and pentagons. These objects contain poles in both μ^2 and the unconstrained component of the loop momenta, t . We are only interested in the coefficient of μ^2 and so series expanding around both $t \rightarrow \infty$ and $\mu^2 \rightarrow \infty$ isolates this single term. For the bubbles a similar procedure applies now in three parameters, a complete description is given in (23).

As in Section 3.1 taking an infinite limit numerically is difficult to do. Similar to the numerical approach to the computation of the cut-containing terms described in Sect. 3.1, we can adapt Badger’s method. This is the approach implemented within `BlackHat` (10). Starting from eq. (45) we “clean” the complex μ plane by subtracting all pentagons at their poles. We then perform a discrete Fourier projection in μ to extract the rational contribution r_3 . For the rational contribution of a triangle we consider the triple cut expression and then clean the complex μ plane by subtracting all terms with an additional propagator. Each such term has a pole in t and its numerator is a quadruple cut. Here we are subtracting the quadruple cut residue of the additional propagator and not the integrand box and pentagon terms, as we would in the OPP approaches. We sidestep therefore any loss of numerical stability that would arise from cancellations between these box and pentagon terms since these pieces are never separated out in the quadruple

cut. The computation of the rational contribution from the two-particle cut of a bubble follows along a similar line.

4 On-Shell Recursion at One Loop

As above, an alternative approach to obtain the full amplitude is to use four-dimensional unitarity methods for the cut-constructible terms and to use recursion relations for the purely rational remainder. The recursive approach developed in Refs. (8, 9) has already been reviewed extensively in (3). While this approach is very useful for analytical calculations and even allows to obtain closed-form all-multiplicity results (65), it is not straightforward to cast into a form suitable for numerical implementation. This is due to the removal of spurious singularities via the introduction of overlap terms, which is difficult to perform in an automated fashion. The approach has subsequently been modified to allow efficient numerical implementation into the automated C++ library `BlackHat` (10). We will discuss here this modified approach, for amplitudes with massless particles in the loop.

We begin by dividing the amplitude into cut-constructible and rational terms, as in eq. (16). The rational terms are defined by setting all scalar integrals to zero,

$$A_n^{1\text{-loop}} = \sum_{j \in B_4} c_j^{D=4} \mathcal{I}_j^D + \mathcal{R}_n, \quad (46)$$

$$C_n \equiv \sum_{j \in B_4} c_j^{D=4} \mathcal{I}_j^D, \quad \mathcal{R}_n \equiv A_n^{1\text{-loop}} \Big|_{\mathcal{I}_j^D \rightarrow 0}. \quad (47)$$

In the following we assume that the cut-containing terms have been computed via the generalized unitarity methods described in the previous section.

The basic idea is to complex continue \mathcal{R} and use Cauchy's theorem to reconstruct the rational term from its poles in the complex plane, similarly to the tree-level approach introduced in Section 2.2. We add this rational term to the previously-computed cut terms C to obtain the full physical amplitude at $z = 0$. However, two of the basic premises of the derivation in Section 2.2 do not hold in general at one loop: For one, we cannot always find shifts (10) such that the amplitude vanishes as $z \rightarrow \infty$. And for another, the division of the amplitude into cut and rational parts introduces the presence of spurious, unphysical poles in the complex plane when considering the rational part separately. That is, the rational part has the following form upon complex continuation,

$$\mathcal{R}_n(z) = \mathcal{R}_n^P(z) + \mathcal{R}_n^S(z) + \mathcal{R}_n^{\text{large } z}, \quad (48)$$

where \mathcal{R}_n^P denotes the contribution from physical poles, which are as at the tree level simple poles, whereas the spurious poles can be simple or double poles, and

the contributions $\mathcal{R}_n^{\text{large } z}$ display polynomial growth in z :

$$\begin{aligned}\mathcal{R}_n^P(z) &= \sum_{\alpha} \frac{A_{\alpha}}{z - z_{\alpha}}, \\ \mathcal{R}_n^S(z) &= \sum_{\beta} \left(\frac{B_{\beta}}{(z - z_{\beta})^2} + \frac{C_{\beta}}{z - z_{\beta}} \right), \\ \mathcal{R}_n^{\text{large } z} &= \sum_{\sigma=0}^{\sigma_{\max}} D_{\sigma} z^{\sigma}.\end{aligned}\tag{49}$$

Here, A, B, C , and D are functions of the external momenta. We postpone the case where $\mathcal{R}_n^P(z)$ has a more complicated structure to Section 4.2.

The physical contribution is recursively computed as in the tree level case,

$$\begin{aligned}- \sum_{\text{poles } \alpha} \text{Res}_{z=z_{\alpha}} \frac{\mathcal{R}_n^P(z)}{z} &= \sum_{r,s} \sum_h \left\{ A_L^h(z = z_{rs}) \frac{i}{K_{r\dots s}^2} \mathcal{R}_R^{-h}(z = z_{rs}) \right. \\ &\quad + \mathcal{R}_L^h(z = z_{rs}) \frac{i}{K_{r\dots s}^2} A_R^{-h}(z = z_{rs}) \\ &\quad \left. + A_L^h(z = z_{rs}) \frac{i\mathcal{F}(K_{r\dots s}^2)}{K_{r\dots s}^2} A_R^{-h}(z = z_{rs}) \right\}.\end{aligned}\tag{50}$$

Here, we have expressed the rational term as a sum of products of rational terms from lower-point amplitudes (defined according to eq. (47)) with lower-point tree amplitudes. The last term with \mathcal{F} corresponds to a one-loop correction to the propagator. Eq. (50) is illustrated in Fig. 5.

The full amplitude is found by combining all rational and cut contributions,

$$A_n^{1\text{-loop}}(0) = C_n(0) - \sum_{\text{poles } \alpha} \text{Res}_{z=z_{\alpha}} \frac{\mathcal{R}_n^P(z)}{z} + \mathcal{R}_n^S(0) + \mathcal{R}_n^{\text{large } z}.\tag{51}$$

We will now show how to obtain the last two contributions, starting with the spurious pole contribution.

4.1 Spurious Poles

The division into cut and rational parts introduces spurious singularities in each of these terms which however cancel in the full amplitude. These spurious singularities are already present in real kinematics. Cauchy's theorem requires us to sum over all poles, whether physical or unphysical. In Ref. (9) this problem was remedied by adding additional rational terms to the cut part. These rational terms are constructed such that the cut and the rational parts individually do not contain spurious singularities upon continuation into the complex plane. However, these extra rational terms then contribute additional terms to the residues at the physical poles in eq. (50) which have to be subtracted from the rational part \mathcal{R} in the recursive construction by so-called overlap terms in order to avoid double counting (9). This approach leads to compact expressions in analytical calculations but is not particularly amenable to numerical implementation.

An alternative way of dealing with the spurious singularities is to make use of the fact that we know that they cancel in the full amplitude. In other words, we can extract the spurious residues from the known cut parts,

$$\mathcal{R}_n^S(0) = - \sum_{\text{spur poles } \beta} \text{Res}_{z=z_\beta} \frac{\mathcal{R}_n^S(z)}{z} = + \sum_{\text{spur poles } \beta} \text{Res}_{z=z_\beta} \frac{C_n(z)}{z}, \quad (52)$$

where $C_n(z)$ is the complex continued cut part. The spurious poles in $C_n(z)$ come from the vanishing of complex continued Gram determinants, $\Delta(z)$, associated with bubble, triangle, and box integrals. Since the spurious poles cancel between the rational and the cut parts, the spurious contribution to the residues from the cut part can only be rational. To compute the residue we therefore series expand the logarithms and polylogarithms around the location of the vanishing Gram determinants and obtain a series of rational functions. The spurious contribution is thus given by evaluating

$$\mathcal{R}_n^S(0) = \sum_{\Delta_m(z_\beta)=0} \text{Res}_{z=z_\beta} \left[\sum_j \frac{c_j^{D=4}(z) \mathcal{I}_j^D(z) \Big|_{\text{rat}}}{z} \right] \equiv \sum_{\Delta_m(z_\beta)=0} \text{Res}_{z=z_\beta} \frac{E_n^\beta(z)}{z}, \quad (53)$$

where the subscript “rat” indicates that we take the rational part of the series expansion of the integrals around the spurious poles. We have introduced the abbreviation E_n^β for these rational terms. The spurious poles z_β are located where the shifted Gram determinants vanish, $\Delta_m(z_\beta) = 0$, with $m = 2, 3, 4$ for bubble, triangle, and box integrals, respectively. Note that poles in Gram determinants of box integrals will in general also appear in the daughter triangle and bubble integrals³. Singularities in triangle integrals will feed down into the daughter bubble coefficients, but not affect the parent box integrals.

The expansion of an integral around the location where its Gram determinant vanishes can be obtained (66) by using the “dimension-shifting relation” (53) iteratively,

$$\mathcal{I}_j^D = \frac{1}{2} \left(\sum_{i=1}^j c_i \mathcal{I}_{j-1}^D[i] + (j-1-D)c_0 \mathcal{I}_j^{D+2} \right), \quad (54)$$

where $\mathcal{I}_{j-1}^D[i]$ denotes the lower-point integral obtained from \mathcal{I}_j^D by removing the i th propagator. The coefficients c_i and c_0 are given by

$$c_i = \sum_{k=1}^j (Y^{-1})_{ik}, \quad c_0 = \sum_{k=1}^j c_k \sim \Delta_j, \quad (55)$$

where Y^{-1} denotes the inverse of the modified Cayley matrix. These modified Cayley matrices are listed for example in (54). As indicated, the coefficient c_0 is proportional to the Gram determinant. We obtain the series expansion of \mathcal{I}_j^D in

³By daughter integrals we mean integrals that can be found from the parent integral by collapsing one or more of the loop propagators.

terms of its Gram determinant,

$$\mathcal{I}_j^D \Big|_{\text{rat}} = \sum_{k=0} r_k \Delta_j^k, \quad (56)$$

with rational coefficients r_k that are found by using eq. (54) iteratively. The explicit expression for the rational expansion of the three-mass triangle is listed in Ref. (10). Similar expansions for the remaining integrals can be obtained as described above and will be listed in a forthcoming publication (C.F. Berger et al., in preparation).

Numerically, we can evaluate eq. (53) by using a discrete Fourier sum, which here only approximates the contour integral. We evaluate the quantity given in the square bracket of (53), $E_n^\beta(z)/z$, at m points equally spaced around a circle of radius δ_β in the z plane, centered on the pole location z_β ,

$$\mathcal{R}_n^S(0) \approx \frac{1}{m} \sum_{\beta} \sum_{j=1}^m \delta_\beta e^{2i\pi j/m} \frac{E_n^\beta(z_\beta + \delta_\beta e^{2i\pi j/m})}{z_\beta + \delta_\beta e^{2i\pi j/m}}. \quad (57)$$

The sum over β runs over all locations of spurious poles where Gram determinants vanish. For technical details of the numerical implementation we refer the reader to Ref. (10).

4.2 Contribution from Infinity

The remaining rational contribution $\mathcal{R}_n^{\text{large } z}$ is the boundary contribution in the contour integral as $z \rightarrow \infty$. Although it is generically possible to find complex continuations that have vanishing boundary contributions, these shifts have in general additional contributions that cannot be constructed recursively as in eq. (50), that is, we have instead,

$$\mathcal{R}_n^P(0) = \mathcal{R}_n^{P \text{ recursive}} + \mathcal{R}_n^{P \text{ nonstd}}, \quad \mathcal{R}_n^{P \text{ recursive}} \equiv - \sum_{\text{poles } \beta} \text{Res}_{z=z_\beta} \frac{\mathcal{R}_n^P(z)}{z}. \quad (58)$$

These ‘non-standard’ contributions (labeled by the superscript ‘nonstd’) arise in configurations where two external momenta with the same helicity are on one side of the partition and all other legs are on the other side. The complex factorization properties of these configurations are not yet fully understood. The sum over poles β in eq. (58) is *only* over the channels that factorize, i. e. that do not display the aforementioned problematic behavior. Conversely, it is possible to find shifts that avoid these ‘non-standard channels’, however, at the price of reintroducing a boundary contribution.

The solution to this problem, developed in Ref. (9), is to use two independent complex continuations to determine the boundary contribution. Let us denote the primary shift by $[j, l]$ and the auxiliary shift by $[a, b]$ in the notation of eq. (10). We then have two relations for the same amplitude, analogous to eq. (51),

$$A_n^{1\text{-loop}}(0) = \text{Inf}_{[j,l]} A_n^{1\text{-loop}} + C_n(0) - \text{Inf}_{[j,l]} C_n + \mathcal{R}_n^{P \text{ recursive}, [j,l]} + \mathcal{R}_n^S [j,l](0), \quad (59)$$

$$A_n^{1\text{-loop}}(0) = C_n(0) - \text{Inf}_{[a,b]} C_n + \mathcal{R}_n^{P \text{ recursive}, [a,b]} + \mathcal{R}_n^{P \text{ nonstd}, [a,b]} + \mathcal{R}_n^S [a,b](0). \quad (60)$$

We have indicated with additional superscripts which shift has been employed. \mathcal{R}_n^S is evaluated according to eq. (53). We have also used that,

$$\mathcal{R}_n^{\text{large } z} = \text{Inf}_{[j,l]} A_n^{1\text{-loop}} - \text{Inf}_{[j,l]} C_n, \quad (61)$$

where $\text{Inf}_{[j,l]} A$ is the unknown large- z behavior of the full amplitude found from a Laurent expansion of $A_n^{1\text{-loop}}(z)$ around $z = \infty$ with the shift $[j, l]$, and similarly for $C_n(z)$. Eqs. (59) and (60) thus both contain unknown terms. If we now apply the primary shift $[j, l]$ to the auxiliary recursion (60), and take the limit $z \rightarrow \infty$, we can extract the large- z behavior of the primary shift,

$$\text{Inf}_{[j,l]} A_n^{1\text{-loop}} = \text{Inf}_{[j,l]} C_n - \text{Inf}_{[j,l]} \left(\text{Inf}_{[a,b]} C_n \right) + \text{Inf}_{[j,l]} \left(\mathcal{R}_n^{P \text{ recursive}, [a,b]} \right) + \text{Inf}_{[j,l]} \left(\mathcal{R}_n^S [a,b](0_{[a,b]}) \right), \quad (62)$$

where now all terms on the right-hand side are either known or recursively constructible, *if*

$$\text{Inf}_{[j,l]} \left(\mathcal{R}_n^{P \text{ nonstd}, [a,b]} \right) = 0. \quad (63)$$

Putting everything together, we find the full amplitude from eq. (59), with (50), (53), and (62), and the cut terms constructed as described in the previous section.

5 Conclusions and Outlook

In this review we have presented an overview of recent developments in the calculation of multi-parton scattering amplitudes at the one-loop level. These developments are based on on-shell techniques that make efficient use of the physical properties of the hard scattering, such as unitarity and factorization. The basic ingredients in these new approaches are on-shell tree-level or lower-point one-loop amplitudes instead of Feynman diagrams, thus sidestepping many of the complications associated with the use of Feynman diagrams.

Furthermore, these new techniques allow for efficient algorithmic implementation and hence the construction of efficient, numerically stable, and fast computer codes, such as `BlackHat` (10), `CutTools/OneLoop` (25, 26), `Rocket` (27), and others (28). With these new techniques and computer tools a flurry of results relevant for the LHC has recently been computed (31, 32, 33, 34, 35, 36), and we expect further rapid progress in the near future.

Nevertheless, much work remains to be done to bring one-loop calculations to the same level of automatization as tree-level computations, ideally starting from a Lagrangian and producing complete events including parton shower and hadronization corrections. Further open issues include, for example, a better

understanding of the complex factorization properties of one-loop amplitudes and the generalization of the new techniques to higher loops in nonsupersymmetric theories.

In summary, the last few years have seen an unprecedented progress in the development of techniques for the computation of multi-parton one-loop scattering amplitudes which are an essential ingredient in precision calculations for the LHC. These new methods have also been used to study the higher-loop structure of $\mathcal{N} = 4$ supersymmetric Yang-Mills theory and $\mathcal{N} = 8$ supergravity (67). Their basic ingredients are unitarity, factorization and complex analysis, properties that are quite generic. It is thus not inconceivable that these new techniques will find further application beyond those presented or referenced in this review.

Acknowledgments

We would like to thank Zvi Bern, Lance Dixon, Fernando Febres Cordero, Tanju Gleisberg, Harald Ita, David Kosower, and Daniel Maître for fruitful collaboration. We also thank Zvi Bern and Lance Dixon for valuable comments. CFB thanks the Aspen Center for Physics for hospitality. This work is supported in part by funds provided by the U.S. Department of Energy under cooperative research agreement DE-FC02-94ER40818.

LITERATURE CITED

1. Bern Z, *et al.* [NLO Multileg Working Group], arXiv:0803.0494 [hep-ph].
2. Reiter T, arXiv:0903.0947 [hep-ph];
Bredenstein A, Denner A, Dittmaier S, Pozzorini S, Phys. Rev. Lett. **103**:012002 (2009) [arXiv:0905.0110 [hep-ph]];
Binoth T, et al., arXiv:0910.4379.
3. Bern Z, Dixon LJ, Kosower DA, Annals Phys. **322**:1587 (2007) [arXiv:0704.2798 [hep-ph]].
4. Bern Z, Dixon LJ, Dunbar DC, Kosower DA, Nucl. Phys. B **425**:217 (1994) [arXiv:hep-ph/9403226];
Bern Z, Dixon LJ, Dunbar DC, Kosower DA, Nucl. Phys. B **435**:59 (1995) [arXiv:hep-ph/9409265].
5. Bern Z, Dixon LJ, Kosower DA, Nucl. Phys. B **513**:3 (1998) [arXiv:hep-ph/9708239].
6. Britto R, Cachazo F, Feng B, Nucl. Phys. B **715**:499 (2005) [arXiv:hep-th/0412308];
Britto R, Cachazo F, Feng B, Witten E, Phys. Rev. Lett. **94**:181602 (2005) [arXiv:hep-th/0501052].
7. Berends FA, Giele WT, Nucl. Phys. B **306**:759 (1988).
8. Bern Z, Dixon LJ, Kosower DA, Phys. Rev. D **73**:065013 (2006) [arXiv:hep-ph/0507005].
9. Berger CF, et al., Phys. Rev. D **74**:036009 (2006) [arXiv:hep-ph/0604195].
10. Berger CF, et al., Phys. Rev. D **78**:036003 (2008) [arXiv:0803.4180 [hep-ph]].
11. Brandhuber A, Spence BJ, Travaglini G, Nucl. Phys. B **706**:150 (2005) [arXiv:hep-th/0407214];
Bedford J, Brandhuber A, Spence BJ, Travaglini G, Nucl. Phys. B **706**:100 (2005) [arXiv:hep-th/0410280];
Bedford J, Brandhuber A, Spence BJ, Travaglini G, Nucl. Phys. B **712**:59 (2005) [arXiv:hep-th/0412108];
Brandhuber A, Spence BJ, Travaglini G, JHEP **0702**:088 (2007) [arXiv:hep-th/0612007].
12. Britto R, Cachazo F, Feng B, Nucl. Phys. B **725**:275 (2005) [arXiv:hep-th/0412103].
13. Ossola G, Papadopoulos CG, Pittau R, Nucl. Phys. B **763**:147 (2007) [arXiv:hep-ph/0609007].
14. Mastrolia P, Ossola G, Papadopoulos CG, Pittau R, JHEP **0806**:030 (2008) [arXiv:0803.3964 [hep-ph]].
15. Forde D, Phys. Rev. D **75**:125019 (2007) [arXiv:0704.1835 [hep-ph]].
16. Britto R, Cachazo F, Feng B, Phys. Rev. D **71**:025012 (2005) [arXiv:hep-th/0410179];
Britto R, Buchbinder E, Cachazo F, Feng B, Phys. Rev. D **72**:065012 (2005)

- [arXiv:hep-ph/0503132].
17. Britto R, Feng B, Mastrolia P, Phys. Rev. D **78**:025031 (2008) [arXiv:0803.1989 [hep-ph]].
 18. Britto R, Feng B, JHEP **0802**:095 (2008) [arXiv:0711.4284 [hep-ph]];
Britto R, Feng B, Yang G, JHEP **0809**:089 (2008) [arXiv:0803.3147 [hep-ph]].
 19. Britto R, Feng B, Phys. Lett. B **681**:376 (2009) [arXiv:0904.2766 [hep-th]].
 20. Mastrolia P, Phys. Lett. B **678**:246 (2009) [arXiv:0905.2909 [hep-ph]];
Mastrolia P, arXiv:0906.3789 [hep-ph].
 21. Giele WT, Kunszt Z, Melnikov K, JHEP **0804**:049 (2008) [arXiv:0801.2237 [hep-ph]].
 22. Bern Z, Morgan AG, Nucl. Phys. B **467**:479 (1996) [arXiv:hep-ph/9511336].
 23. Badger SD, JHEP **0901**:049 (2009) [arXiv:0806.4600 [hep-ph]].
 24. Ossola G, Papadopoulos CG, Pittau R, JHEP **0805**:004 (2008) [arXiv:0802.1876 [hep-ph]];
Draggiotis P, Garzelli MV, Papadopoulos CG, Pittau R, JHEP **0904**:072 (2009) [arXiv:0903.0356 [hep-ph]].
 25. Ossola G, Papadopoulos CG, Pittau R, JHEP **0803**:042 (2008) [arXiv:0711.3596 [hep-ph]].
 26. van Hameren A, Papadopoulos CG, Pittau R, JHEP **0909**:106 (2009) [arXiv:0903.4665 [hep-ph]].
 27. Ellis RK, et al., JHEP **0901**:012 (2009) [arXiv:0810.2762 [hep-ph]].
 28. Lazopoulos A, arXiv:0812.2998 [hep-ph];
Winter, JC, Giele WT, arXiv:0902.0094 [hep-ph]. Kilian W, Kleinschmidt T, arXiv:0912.3495.
 29. Gleisberg T, Krauss F, Eur. Phys. J. C **53**:501 (2008) [arXiv:0709.2881 [hep-ph]];
Gleisberg T, et al., JHEP **0902**:007 (2009) [arXiv:0811.4622 [hep-ph]].
 30. Frederix R, Frixione S, Maltoni F, Stelzer T, JHEP **0910**:003 (2009) [arXiv:0908.4272 [hep-ph]].
 31. Berger CF, et al., Phys. Rev. Lett. **102**:222001 (2009) [arXiv:0902.2760 [hep-ph]];
Berger CF, et al., Phys. Rev. D **80**:074036 (2009) [arXiv:0907.1984 [hep-ph]].
 32. Ellis RK, Melnikov K, Zanderighi G, Phys. Rev. D **80**:094002 (2009) [arXiv:0906.1445 [hep-ph]];
Melnikov K, Zanderighi G, arXiv:0910.3671 [hep-ph].
 33. Melnikov K, Schulze M, JHEP **0908**:049 (2009) [arXiv:0907.3090 [hep-ph]].
 34. Ossola G, Papadopoulos CG, Pittau R, JHEP **0707**:085 (2007) [arXiv:0704.1271 [hep-ph]].
 35. Binoth T, Ossola G, Papadopoulos CG, Pittau R, JHEP **0806**:082 (2008) [arXiv:0804.0350 [hep-ph]].
 36. Bevilacqua G, et al., JHEP **0909**:109 (2009) [arXiv:0907.4723 [hep-ph]].

37. Mangano ML, Parke SJ, Phys. Rept. **200**:301 (1991) [arXiv:hep-th/0509223].
38. Dixon LJ, arXiv:hep-ph/9601359.
39. Bern Z, Dixon LJ, Kosower DA, Ann. Rev. Nucl. Part. Sci. **46**:109 (1996) [arXiv:hep-ph/9602280].
40. Paton JE, Chan HM, Nucl. Phys. B **10**:516 (1969);
Cvitanovic P, Lauwers PG, Scharbach PN, Nucl. Phys. B **186**:165 (1981);
Berends FA, Giele W, Nucl. Phys. B **294**:700 (1987);
Mangano ML, Nucl. Phys. B **309**:461 (1988);
Zeppenfeld D, Int. J. Mod. Phys. A **3**:2175 (1988);
Bern Z, Kosower DA, Nucl. Phys. B **362**:389 (1991);
Del Duca V, Frizzo A, Maltoni F, Nucl. Phys. B **568**:211 (2000) [arXiv:hep-ph/9909464];
Del Duca V, Dixon LJ, Maltoni F, Nucl. Phys. B **571**:51 (2000) [arXiv:hep-ph/9910563];
Maltoni F, Paul K, Stelzer T, Willenbrock S, Phys. Rev. D **67**:014026 (2003) [arXiv:hep-ph/0209271].
41. Kanaki A, Papadopoulos CG, Comput. Phys. Commun. **132**:306 (2000) [arXiv:hep-ph/0002082].
42. Giele W, Kunszt Z, Winter J, arXiv:0911.1962 [Unknown].
43. Kleiss R, Stirling WJ, Nucl. Phys. B **262**:235 (1985).
44. Mangano ML, et al., JHEP **0307**:001 (2003) [arXiv:hep-ph/0206293].
45. Gleisberg T, Höche S, JHEP **0812**:039 (2008) [arXiv:0808.3674 [hep-ph]].
46. Schwinn C, Weinzierl S, JHEP **0704**:072 (2007) [arXiv:hep-ph/0703021];
Badger SD, Glover EWN, Khoze VV, Svrček P, JHEP **0507**:025 (2005) [arXiv:hep-th/0504159];
Badger SD, Glover EWN, Khoze VV, JHEP **0601**:066 (2006) [arXiv:hep-th/0507161].
47. Bedford J, Brandhuber A, Spence BJ, Travaglini G, Nucl. Phys. B **721**:98 (2005) [arXiv:hep-th/0502146];
Cachazo F, Svrček P, arXiv:hep-th/0502160;
Bjerrum-Bohr NEJ, et al., JHEP **0601**:009 (2006) [arXiv:hep-th/0509016];
Benincasa P, Boucher-Veronneau C, Cachazo F, JHEP **0711**:057 (2007) [arXiv:hep-th/0702032];
Brandhuber A, McNamara S, Spence B, Travaglini G, JHEP **0703**:029 (2007) [arXiv:hep-th/0701187];
Elvang H, Freedman DZ, Kiermaier M, JHEP **0904**:009 (2009) [arXiv:0808.1720 [hep-th]];
Elvang H, Freedman DZ, Kiermaier M, JHEP **0906**:068 (2009) [arXiv:0811.3624 [hep-th]].
48. Britto R, et al., Phys. Rev. D **71**:105017 (2005) [arXiv:hep-th/0503198];
Forde D, Kosower DA, Phys. Rev. D **73**:065007 (2006)

- [arXiv:hep-th/0507292];
Drummond JM, Henn JM, JHEP **0904**:018 (2009) [arXiv:0808.2475 [hep-th]].
49. Draggiotis PD, Kleiss RHP, Lazopoulos A, Papadopoulos CG, Eur. Phys. J. C **46**:741 (2006) [arXiv:hep-ph/0511288];
Vaman D, Yao YP, JHEP **0604**:030 (2006) [arXiv:hep-th/0512031];
Arkani-Hamed N, Kaplan J, JHEP **0804**:076 (2008) [arXiv:0801.2385 [hep-th]];
Cheung C, arXiv:0808.0504 [hep-th];
Feng B, Wang J, Wang Y, Zhang Z, arXiv:0911.0301 [hep-th].
50. Mason L, Skinner D, arXiv:0903.2083 [hep-th];
Hodges A, arXiv:0905.1473 [hep-th];
Arkani-Hamed N, Cachazo F, Cheung C, Kaplan J, arXiv:0907.5418 [hep-th];
Arkani-Hamed N, Cachazo F, Cheung C, arXiv:0909.0483 [hep-th];
Mason L, Skinner D, JHEP **0911**:045 (2009) [arXiv:0909.0250 [hep-th]];
Bullimore M, Mason L, Skinner D, arXiv:0912.0539 [hep-th];
Kaplan J, arXiv:0912.0957;
Arkani-Hamed N, Bourjaily J, Cachazo F, Trnka J, arXiv:0912.3249.
51. Brown LM, Feynman RP, Phys. Rev. **85**:231 (1952);
Melrose DB, Nuovo Cim. **40**:181 (1965);
Passarino G, Veltman MJG, Nucl. Phys. B **160**:151 (1979);
Stuart RG, Comput. Phys. Commun. **48**, 367 (1988);
van Oldenborgh GJ, Vermaseren JAM, Z. Phys. C **46**:425 (1990);
Pittau R, Comput. Phys. Commun. **104**:23 (1997) [arXiv:hep-ph/9607309];
Pittau R, Comput. Phys. Commun. **111**:48 (1998) [arXiv:hep-ph/9712418];
Weinzierl S, Phys. Lett. B **450**:234 (1999) [arXiv:hep-ph/9811365].
52. van Neerven WL, Vermaseren JAM, Phys. Lett. B **137**, 241 (1984).
53. Bern Z, Dixon LJ, Kosower DA, Phys. Lett. B **302**:299 (1993) [Erratum-ibid. B **318**:649 (1993)] [arXiv:hep-ph/9212308];
Bern Z, Dixon LJ, Kosower DA, Nucl. Phys. B **412**:751 (1994) [arXiv:hep-ph/9306240].
54. Ellis RK, Zanderighi G, JHEP **0802**:002 (2008) [arXiv:0712.1851 [hep-ph]].
55. Risager K, arXiv:0804.3310 [hep-th].
56. Cachazo F, arXiv:0803.1988 [hep-th].
57. Bjerrum-Bohr NEJ, Dunbar DC, Perkins WB, JHEP **0804**:038 (2008) [arXiv:0709.2086 [hep-ph]].
58. Bern Z, Bjerrum-Bohr NEJ, Dunbar DC, Ita H, Nucl. Phys. Proc. Suppl. **157**:120 (2006) [arXiv:hep-ph/0603187].
59. Kilgore WB, arXiv:0711.5015 [hep-ph].
60. Ellis RK, Giele WT, Kunszt Z, Melnikov K, Nucl. Phys. B **822**:270 (2009) [arXiv:0806.3467 [hep-ph]].

61. Ellis RK, Giele WT, Kunszt Z, JHEP **0803**:003 (2008) [arXiv:0708.2398 [hep-ph]].
62. W. L. van Neerven, Nucl. Phys. B **268**, 453 (1986).
63. Anastasiou C, et al., JHEP **0703**:111 (2007) [arXiv:hep-ph/0612277].
64. Garzelli MV, Malamos I, Pittau R, arXiv:0910.3130 [hep-ph].
65. Forde D, Kosower DA, Phys. Rev. D **73**, 061701 (2006) [arXiv:hep-ph/0509358];
Berger CF, et al., Phys. Rev. D **75**:016006 (2007) [arXiv:hep-ph/0607014];
Berger CF, Del Duca V, Dixon LJ, Phys. Rev. D **74**:094021 (2006) [Erratum-ibid. D **76**:099901 (2007)] [arXiv:hep-ph/0608180];
Badger SD, Glover EWN, Risager K, JHEP **0707**:066 (2007) [arXiv:0704.3914 [hep-ph]].
66. Campbell JM, Glover EWN, Miller DJ, Nucl. Phys. B **498**:397 (1997) [arXiv:hep-ph/9612413];
Giele WT, Glover EWN, JHEP **0404**:029 (2004) [arXiv:hep-ph/0402152];
Giele W, Glover EWN, Zanderighi G, Nucl. Phys. Proc. Suppl. **135**:275 (2004) [arXiv:hep-ph/0407016].
67. Bern Z, Dixon LJ, Smirnov VA, Phys. Rev. D **72**:085001 (2005) [arXiv:hep-th/0505205];
Bern Z, et al., Phys. Rev. D **77**:025010 (2008) [arXiv:0707.1035 [hep-th]];
Arkani-Hamed N, Cachazo F, Kaplan J, arXiv:0808.1446 [hep-th];
Bern Z, et al., Phys. Rev. Lett. **103**:081301 (2009) [arXiv:0905.2326 [hep-th]].

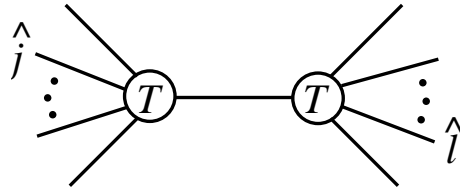


Figure 1: Schematic representation of a typical tree recursive contribution to eq. (14). The labels ‘ T ’ refer to on-shell tree amplitudes. The momenta \hat{j} and \hat{l} are complex continued, on-shell momenta.

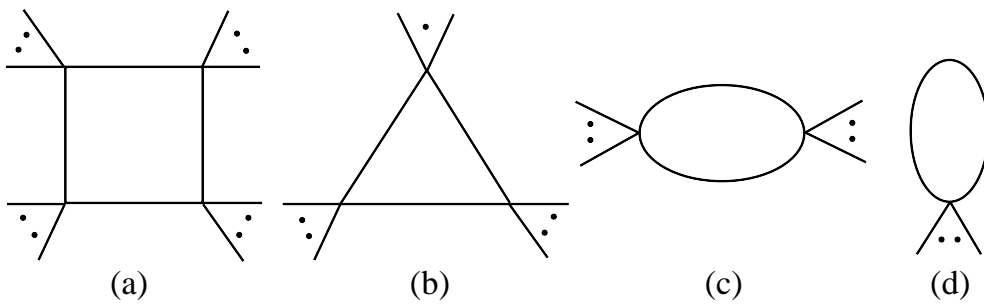


Figure 2: Representative examples of integrals appearing in eq. (16): (a) a box integral, that is, a 4-point integral, (b) a triangle (3-point) integral, (c) a bubble (2-point) integral, and (d) a tadpole integral. Each corner can have one or more external momenta attached to it. The tadpole vanishes when all internal propagators are massless.

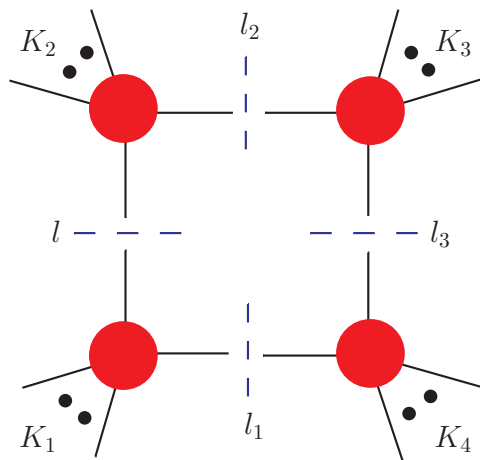


Figure 3: A quadruple cut one-loop integral isolating the single box term $d_0(K_1^2, K_2^2, K_3^2, K_4^2)$.

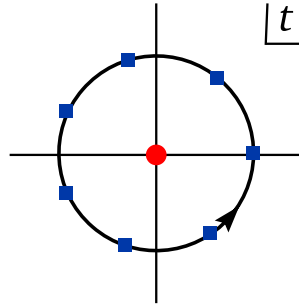


Figure 4: The points on the circle used by the discrete Fourier projection, cf. eq. (24).

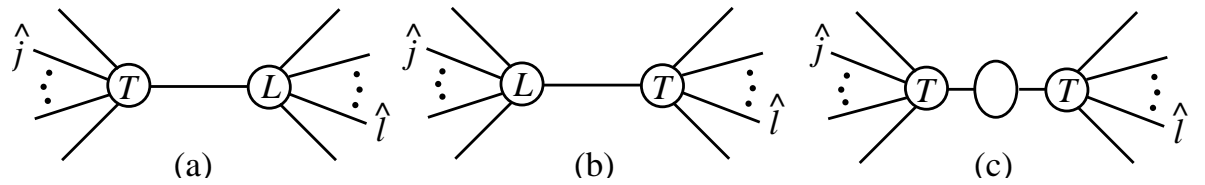


Figure 5: Schematic representation of one-loop recursive contributions to eq. (50). The labels ‘T’ and ‘L’ refer to tree and the rational part of loop vertices, respectively.